# On using regional gravity data to improve inversion of airborne gravity gradiometer data: the G-GG approach.

**Robert Ellis**
*Geosoft Inc.*
*Toronto, Canada*
*Robert.Ellis@Geosoft.com*

**Gaud Pouliquen**
*Geosoft (UK)*
*Oxford, UK*
*Gaud.Pouliquen@Geosoft.com*

**Taronish Pithawala**
*Geosoft Inc.*
*Toronto, Canada*
*Taronish.Pithawala@Geosoft.com*

**Ian MacLeod***
*Geosoft Inc.*
*Toronto, Canada*
*Ian.MacLeod@Geosoft.com*

**presenting author asterisked*

## SUMMARY

Gravity gradiometer data are becoming a frequent and useful aid in revealing the density structure of the earth both for targeting and mapping in exploration programs, particularly with decreasing noise levels and improved processing techniques. We present an inversion method for improving gravity gradiometer survey outcomes when regional gravity data are available. In essence, the gravity gradiometer data supply the smaller spatial wavelength information in the inversion while the gravity data supply the longer wavelength density trends. We demonstrate the method using synthetic data and then on field data from the Kauring test site.

Comparing our gravity referenced gravity gradiometer (G-GG) inversion with conventional practice illustrates two important advantages of the G-GG method: first the locations of compact targets are better estimated; and second, geologic mapping is significantly enhanced.

**Key words:** inversion, gravity, gravity gradients, AGG, G-GG, Kauring.

## INTRODUCTION

The advent of modern airborne gravity gradiometers provides a second window on the density of the earth following the window provided by modern gravimeters. While both systems are sensitive to density variation they have different sensitivities: the gradiometer has a $r^{-3}$ sensitivity while the gravimeter has a $r^{-2}$ sensitivity, where $r$ is the distance between the density source and the sensor location. Consequently, inversion of gradiometer data provides a good smaller wavelength density model while inversion of gravimeter data provides a better larger spatial wavelength density model. Of course this is well-known. What we address in this work is how to combine gradiometer and gravimeter data to produce a density model which contains the full range of spatial wavelengths available from both data types. In view of the nature of the forum we are formulating the problem in terms of how gravity data can be used to improve gravity gradiometer data inversion, however, our more general intent is to illustrate a general method for deriving the optimum exploration model from all available data.

There are many ways to approach the problem of combining gradiometer data and regional gravimeter data, too many to review or critique in this abstract. Instead we present a remarkably simple, general, and effective method which is easy to implement in any inversion workspace, such as provided by Geosoft's VOXI or similar. For convenience we denote our gravity referenced gravity gradient inversion method, G-GG. We demonstrate and explain the G-GG method using synthetic data so that inversion results produced can be compared to the known true model. For the synthetic case we compare G-GG outcomes with "conventional" outcomes, and then demonstrate the G-GG method using Falcon™ Airborne Gravity Gradiometer (AGG) data from the R.J. Smith Kauring Test Range at Kauring, Western Australia, together with ground gravity data sampled on a 500m grid. We will show that by appropriately combining gravimeter inversion with gradiometer inversion we can produce a density model which is truly a case of the whole being better than the sum of the parts.

An alternate view of the problem of combining gravimeter and gradiometer inversion is from the perspective of regional-residual separation for AGG data prior to inversion. In geophysical inversion best practice is to separate the signal from targets contained in the inversion domain from the signal due to structures outside the model domain. Failure to make this separation will yield poor inversion results. Typically, for expediency, a simple linear or quadratic trend is used as a regional-residual separation prior to inversion. We acknowledge of course that proper regional-residual separation is a subject area in itself with many geophysicists dissatisfied with simplistic trend removal; however, the fact remains that proper regional-residual separation is time consuming and challenging and is often substituted with a simple mathematical separation. Using the approach we advocate the regional gravity data in effect automatically provide a very good, geological, AGG regional.

## METHOD AND RESULTS

The most straightforward way of explaining and motivating the G-GG method is by studying a simple model. In the process we will also observe the effect of regional-residual separation in AGG inversion. Consider the simple density model shown in Figure 1 consisting of crystalline host (green, density 2.67 g/cm$^3$) with 200m thick sedimentary cover on the right (blue, density 1.67 g/cm$^3$). A mineralized zone (red, 3.67 g/cm$^3$ 250m x 750m x 100 m$^3$) is buried in the crystalline host on the left. The model is assumed to continue horizontally sufficently beyond the domain of interest to avoid any edge effects in data simulation. All simulated survey results over this model have a 65m clearance and sufficient sampling and line spacing to avoid aliasing and have negligible noise. We assume that a complete Bouguer correction has been applied to all responses with a density of 2.67 g/cm$^3$. We choose these ideal conditions deliberately to focus exclusively on the effects we are trying to illustrate.

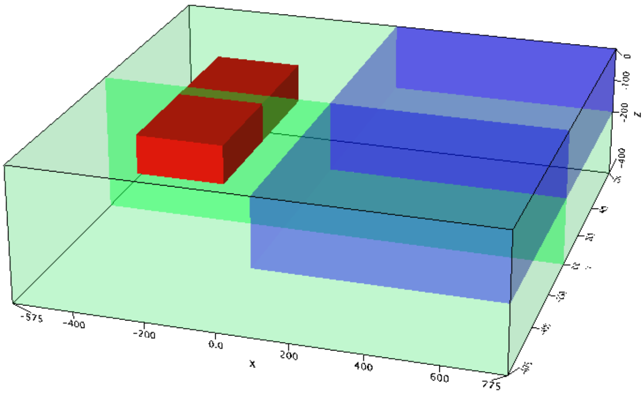


**Figure 1: A density model consisting of a crystalline host (green), a regional sedimentary cover (blue), and a mineralized zone (red), with densities 2.67, 1.67, 3.67 g/cm$^3$ respectively.**

**Inversion 1: Target Only Benchmark**

As a benchmark we first simulate the standard FALCON™ AGG responses ($G_{NE}$ and $G_{UV}$) of the mineralized zone in the crystalline host, i.e., without the sedimentary cover, and then invert the responses to recover a density model. The result of this process is shown in Figure 1.1 as a section through the 3D model corresponding to the section highlighted in Figure 1. In all AGG inversions for this model we enforce a 0.2 Eo RMS fit to the data.

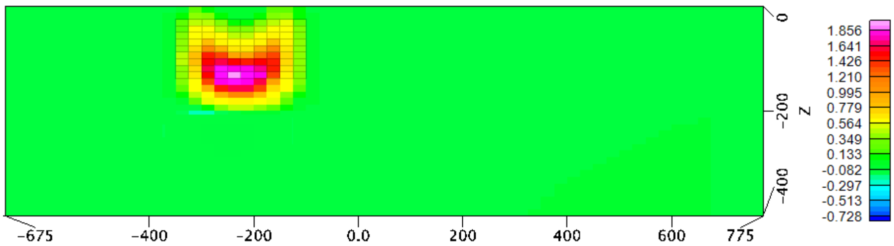


**Figure 1.1: A density (g/cm$^3$) section through the model recovered by inversion of the mineralized zone only response. The section location is shown highlighted in Figure 1. The true target is shown in wireframe.**

The mineralized zone only inversion density section shown in Figure 1.1 demonstrates that inversion of AGG data will recover reasonable representations of compact targets in a uniform host: the geometry and the depth estimates are satisfactory. We note that the recovered depth is a little deeper than the true target due to the lateral extension of the target; a spherical target will be located almost exactly. Next we include the sedimentary cover in to the model.

**Inversion 2: Conventional Gravity Gradient Inversion**

We proceed in the same manner as the previous inversion with the single exception of including the sedimentary cover contribution into the simulated AGG data. The data (in Eo) are shown in Figure 2.1 ($G_{NE}$ left, $G_{UV}$ right). Observe that the $G_{NE}$ data are insensitive the N-S striking sedimentary cover while the $G_{UV}$ data are dominated by it. This is the essence of the problem we are investigating. If we assume we are most interested in estimating the geometry and depth of the mineralized zone we might consider attempting a "regional-residual" separation on the AGG data prior to inversion, in essence trying to remove the "regional" contribution to the AGG data due to the sedimentary cover. The most common approach in practice is to remove a linear trend from each of the AGG input channels prior to inversion. A more modest approach is to remove the mean from each AGG channel. In practice inverting the total response is not viable because systematic gravity gradient channel offset errors are common in today's delivered data (FTG and AGG). Indeed in a Section below we will see this is the case with the AGG data supplied from the Kauring test site.

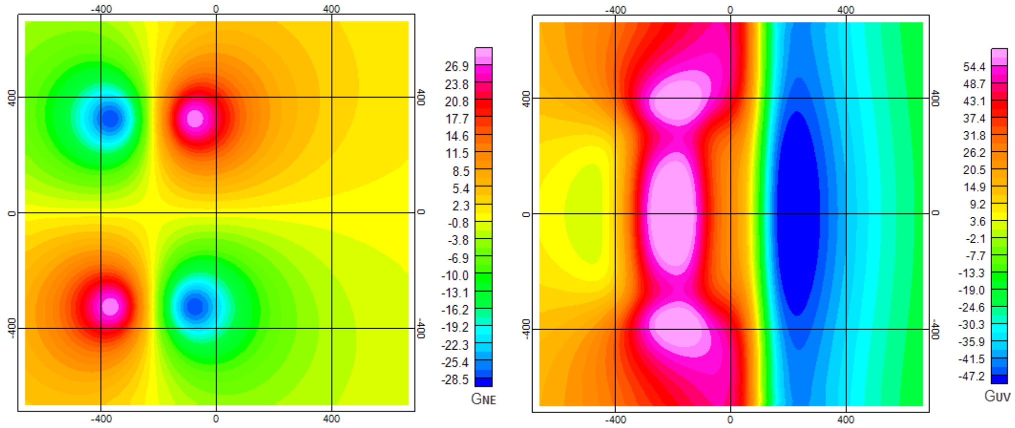


**Figure 2.1: The $G_{NE}$ and $G_{UV}$ (Eo) responses over the model shown in Figure 1.**

The result of inverting the AGG data shown in Figure 2.1 for, first, linear trend removal, and second, mean constant removal are shown in Figures 2.2 and 2.3 respectively for the same section as shown in Figure 1.1. Since this is synthetic data and given the nature of $G_{NE}$ and $G_{UV}$ sensitivities the mean constant removal is 0 Eo and only 3 Eo respectively and provides visually the same inversion result as no trend removal. Both cases indicate a dense zone in the vicinity of the true mineralized zone however they are far from satisfactory from an exploration perspective. The divergence of the results confirms the well-known (but perhaps not well enough attended) impact of regional-residual separation in geophysical data interpretation, and, is a motivation for our use of regional gravity to supply the regional component in AGG inversion.

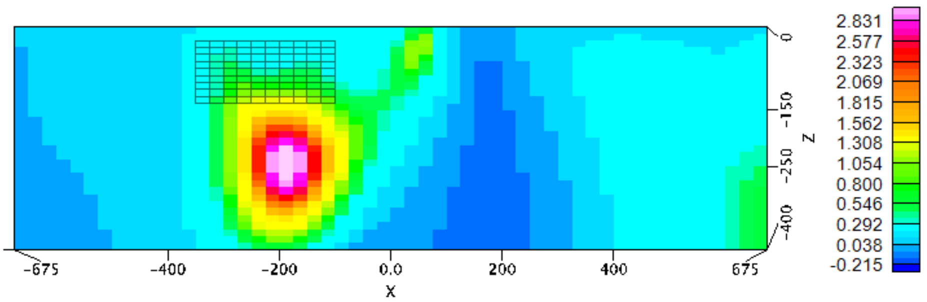


**Figure 2.2: The density (g/cm$^3$) section from the linear-trend-removal inversion of the $G_{NE}$ and $G_{UV}$ data shown in Figure 2.1 The true target is shown in wireframe.**

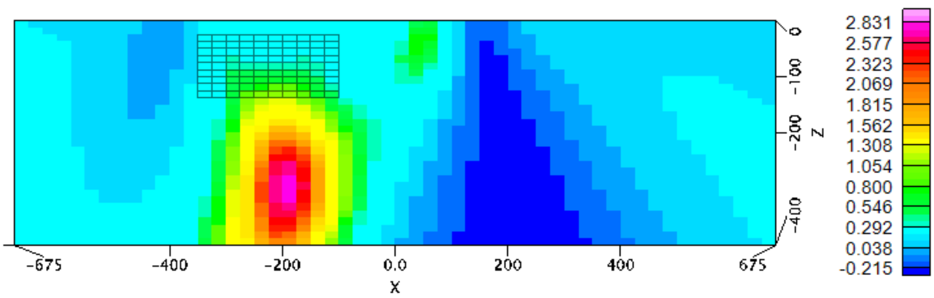


**Figure 2.3: The density (g/cm$^3$) section from the mean-trend-removal inversion of the $G_{NE}$ and $G_{UV}$ data shown in Figure 2.1 The true target is shown in wireframe.**

**Inversion 3: Gravity Referenced Gravity Gradient Inversion**

A linear or quadratic trend background removal on each AGG channel is found to be very effective in practice and is recommended in the absence of any other information that can be used to create a geophysical AGG regional response. One particularly useful source of other information is a regional gravity survey. Inverting the gravity data yields a regional density model which in turn can be used to guide the behaviour of an AGG inversion. A particularly efficient, and in our opinion optimal, inversion approach is to use the regional density model derived from the gravity inversion as the "reference model" for the AGG inversion. Recall that geophysical inversion is ill-posed, meaning in particular in our case, many quite different density models give rise to the same gravity or gravity gradient responses. To provide a single solution in such a situation the inversion must be regularized, that is, a preferred or "reference model" must be specified a priori by the user toward which the inversion result will trend while satisfying a data misfit or other criteria.

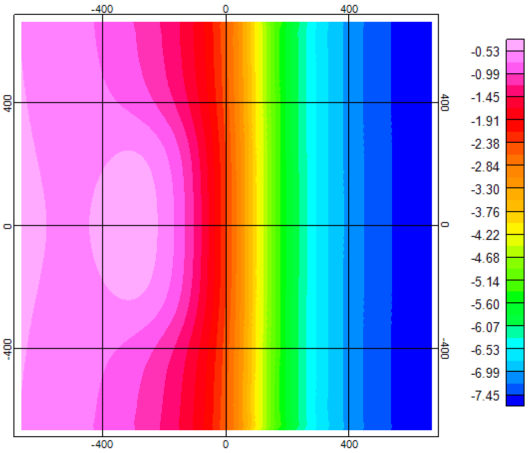


**Figure 3.1: The $G_Z$ (mgal) gravity response over the model shown in Figure 1.**

For the synthetic model in Figure 1 the "regional" gravity response is shown in Figure 3.1. It is straightforward to invert the "regional" gravity data to produce a corresponding regional density model. The result of the inversion is shown in section view in Figure 3.2. As expected the gravity data is sensitive to the bulk density and clearly discriminates between the higher density crystalline host on the left and the less dense sediments on the right. The mineralized zone is also identified but, as is expected with gravity data, the resolution is poor. Fortunately this is an advantage for our approach because we are primarily interested in the regional density model. Next we take the density model from the gravity inversion and use it as a reference model for the AGG inversion where now we need no regional-residual separation, i.e. we invert the total response.

The result of the gravity referenced gravity gradient G-GG inversion is shown in Figure 3.3. The mineralized zone is well located, much better than using a linear trend, a constant, or no background removal prior to inversion (c.f. Figures 2.2 and 2.3). The sediment boundary is also better resolved. The sediment horizontal contact does not contribute to the AGG data: a constant mass layer has zero AGG response.

The G-GG process we have just described is very simple to implement and as shown provides a method for improving gravity gradient inversion when regional gravity data are available. The process can be applied to any airborne gravity gradiometer data (e.g. AGG, FTG or VK data) or any gravity gradient components (e.g. $G_{ZZ}$). It completely decouples the gravity gradient inversion from the gravity inversion which is an important consideration. Joint inversion of gravity and gravity gradient data is mathematically simple however the different sampling densities and error levels make the sequential inversion process we suggest far more efficient and effective in practice. We will now demonstrate the gravity referenced AGG inversion process on data from the Kauring test site.

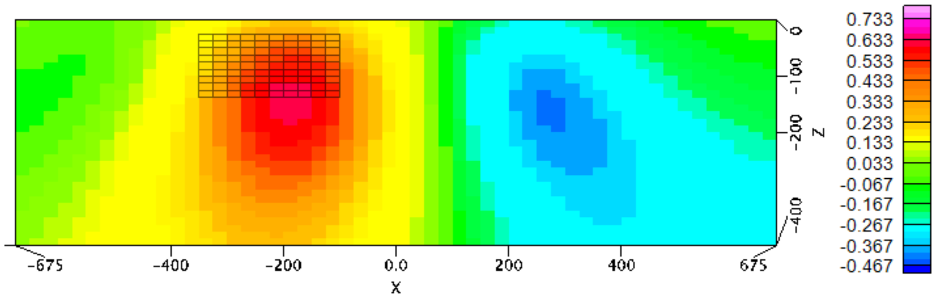


**Figure 3.2: The density (g/cm$^3$) section from the gravity inversion of the $G_Z$ data shown in Figure 3.1 The true target is shown in wireframe, the true sediment contact is at x=100.**

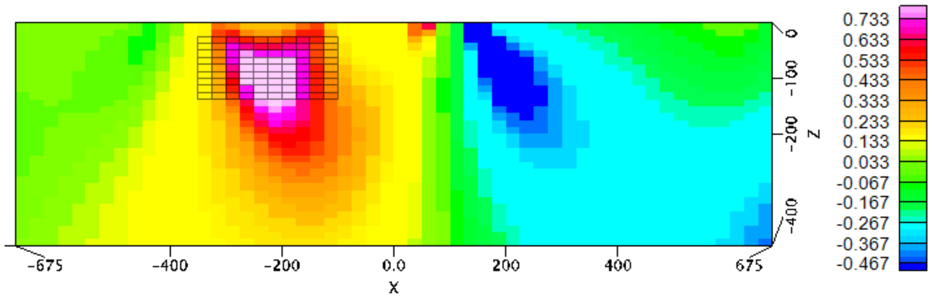


**Figure 3.3 The density (g/cm$^3$) section from the G-GG inversion of the $G_{NE}$ and $G_{UV}$ data shown in Figure 2.1 The true target is shown in wireframe, the true sediment contact is at x=100.**

**Inversion 4: Kauring Conventional Gravity Gradient Inversion**

The Kauring test site has been well described in the literature and to which we refer the interested reader (e.g. Bates & Elieff, 2012, Howard et al, 2010, Lane et al 2009). For our purposes it suffices that there is a high quality Falcon™ AGG survey over the site together with regional gravity sampled on a 500m x 500m grid. We will also assume the reader is familiar with Falcon™ AGG data (Lee 2001). Preparing and processing AGG data is a sophisticated process and beyond the scope of this work to review (Zhdanov et al 2004). In Figures 4.1a-d we show the A/B_2p67_NE/UV channels being the two complements of the gravity gradients delivered by the system (corresponding two measurements of $G_{NE}$ and $G_{UV}$), with the usual corrections, including a 2.67 g/cm$^3$ terrain density correction. Be aware that the data are displayed in a rotated reference frame with N at 30° to the vertical. We note that the standard deviation between the A and B complement data can be used as a guide to the inversion error levels. For the Kauring Falcon™ AGG data the standard deviation of A-B is ~4.5 Eo which under certain statistical assumptions would suggest a ~4/√2 Eo noise on the individual A and B channels. Suffice to say that we choose to fit all inversions to a 3.5 Eo noise level.

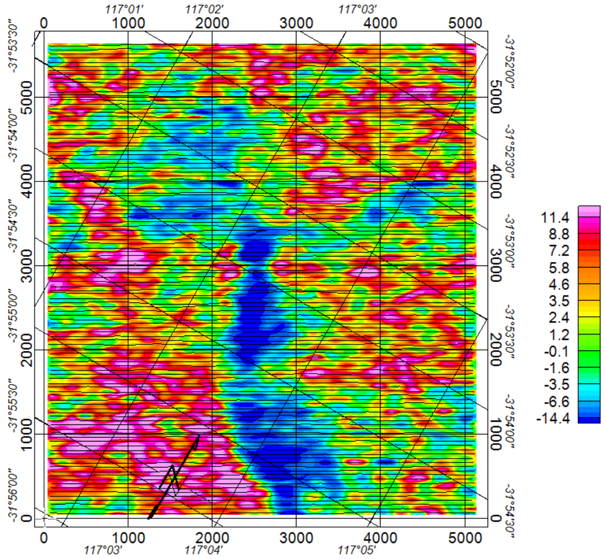


**Figure 4.1a: The Kauring $A_{NE}$ response in Eo.**

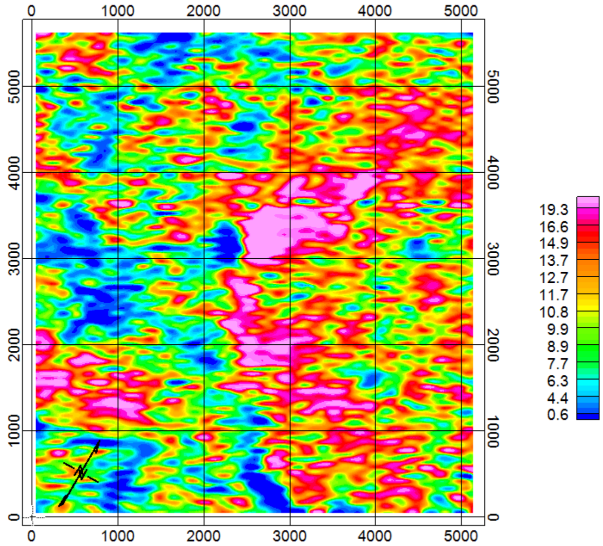


**Figure 4.1b: The Kauring $A_{UV}$ response in Eo.**

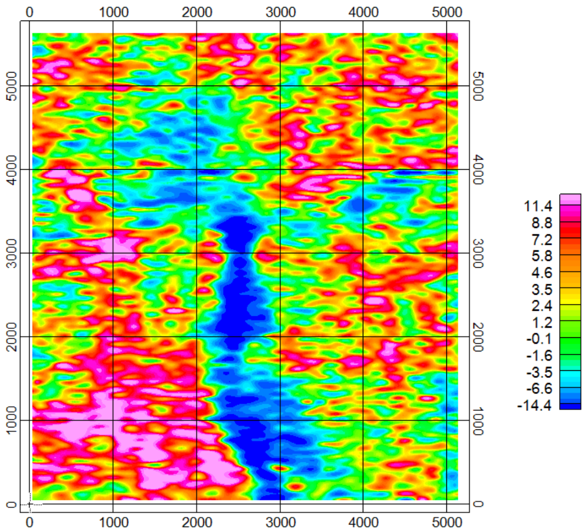


**Figure 4.1c: The Kauring $B_{NE}$ response in Eo.**

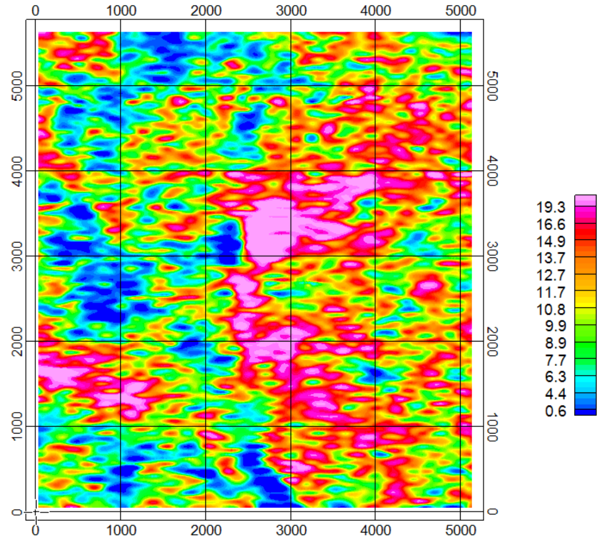


**Figure 4.1d: The Kauring $B_{UV}$ response in Eo.**

As a benchmark we begin with a "conventional" inversion of the A/B_2p67_NE/UV data using the Lidar 10m data to define the DEM and the GPSZ channel to define the sensor location. A "conventional" inversion involves removing a linear trend from all AGG channels before inversion. We call this "conventional" because without this trend removal it will usually be difficult to fit the AGG data and the data misfit will not be reasonably distributed among the 4 input channels. A hint of the importance of this issue can be seen by observing the range of the NE and UV data in Figures 4.1a-d. In general because of the form of the NE and UV gravity gradient sensitivities the data means should be close to zero. Observe that the UV channels have a mean ~10 Eo while the NE mean is ~3 Eo. Since we are jointly inverting these channels they must be mutually consistent or the inversion will fail. Applying a linear trend removal effectively removes components from the data due to sources outside the model domain and also corrects possible processing and systematic errors. It is the experience of the authors that systematic offset errors are present in many delivered gravity gradient survey datasets (FTG and AGG).

The result of the "conventional" inversion is shown in Figures 4.2a-f where the surface density and horizontal sections are shown at 250m, 150m, -150m elevations which correspond approximately to 0m, 100m, 200m and 500m below surface, and a section through the primary density anomaly.

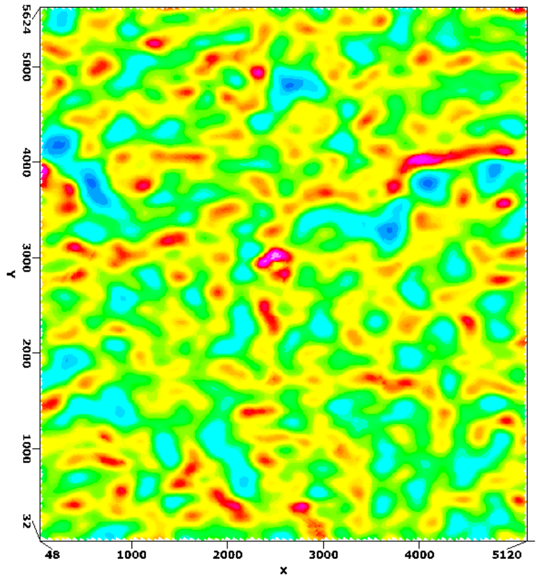


**Figure 4.2a: The surface density (g/cm$^3$) from the conventional linear trend removal AGG inversion.**

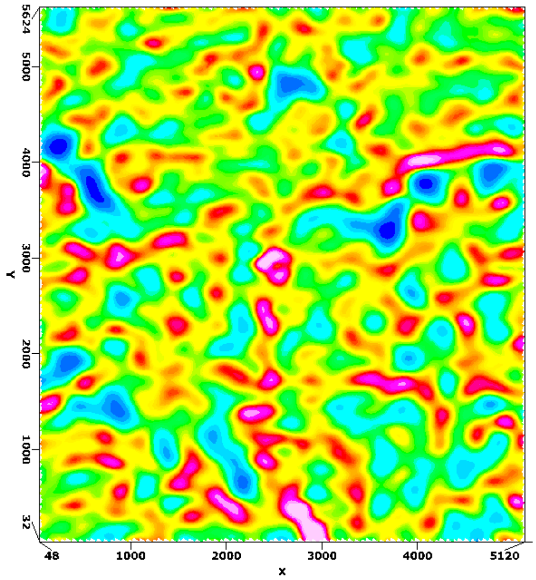


**Figure 4.2b: A density slice at elevation 250m from the conventional AGG inversion.**

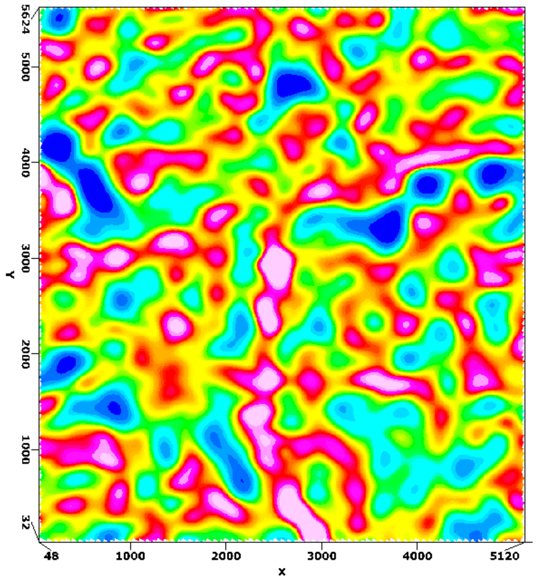


**Figure 4.2c: A density slice at elevation 150m from the conventional AGG inversion.**

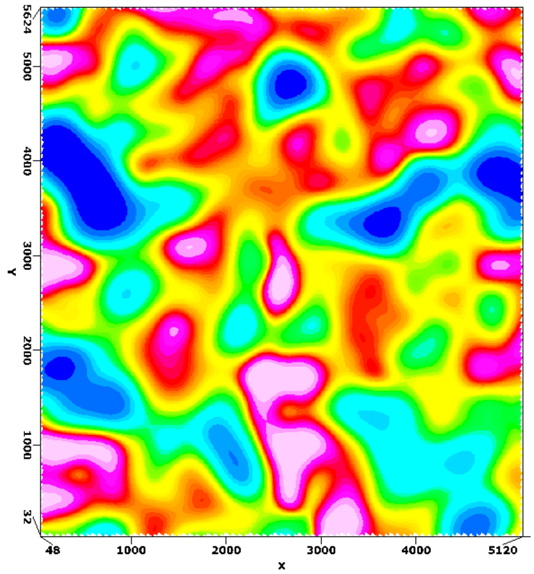


**Figure 4.2d: A density slice at elevation -150m from the conventional AGG inversion.**

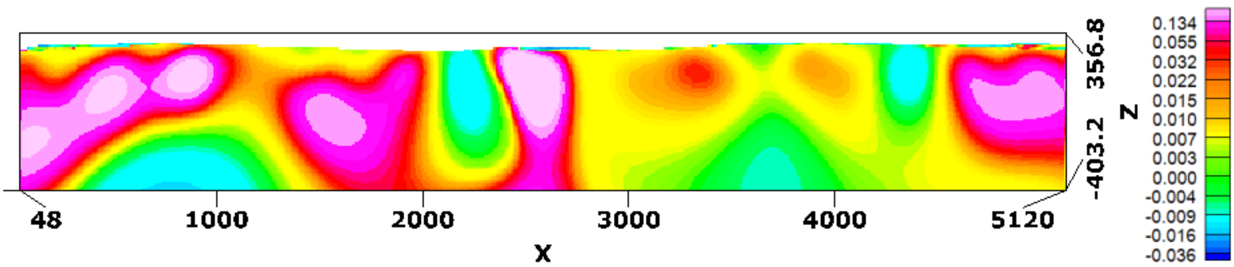


**Figure 4.2e: A section at y=3000m through the density model (g/cm$^3$) produced by the conventional linear trend removal AGG inversion. A histogram equalized colour scale is used to convey the general structure of the model.**

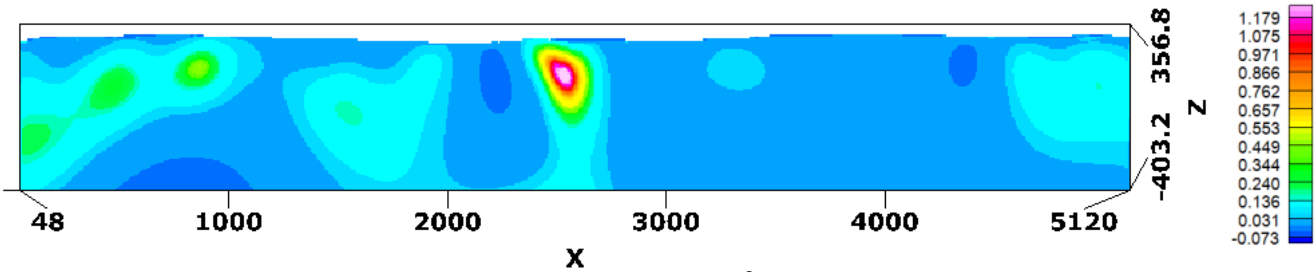


**Figure 4.2f: A section at y=3000m through the density model (g/cm$^3$) produced by the conventional linear trend removal AGG inversion. A linear colour scale is used to convey the structure of the high density target.**

**Inversion 5: Kauring Gravity Referenced Gravity Gradient (G-GG) Inversion**

The regional gravity data at the Kauring site are shown in Figure 5.1. The polygon shows the AGG survey area discussed above. It is straightforward to invert the regional gravity data however we make one exception to the "conventional" inversion: we do not remove a linear trend from the data before inversion, instead only remove the mean of the data. The range of the data indicates a mean ~ -30 mgal. Removing a constant corresponds to a Bouguer slab correction prior to inversion. We do not remove the linear trend because we wish to have the gravity model supply the long wavelength behaviour for the AGG inversion.

Inverting the gravity data yields the result shown in Figure 5.2 where we have partially exposed a section of the gravity model under line (dashed) at y=3000 in the rotated coordinate system. The results are quite straightforward: the NW-SE trending structure is visible in the both the gravity data and in the inversion model; and the inversion model shows a higher density domain in the SW corner trending toward lower density in the NE corner.

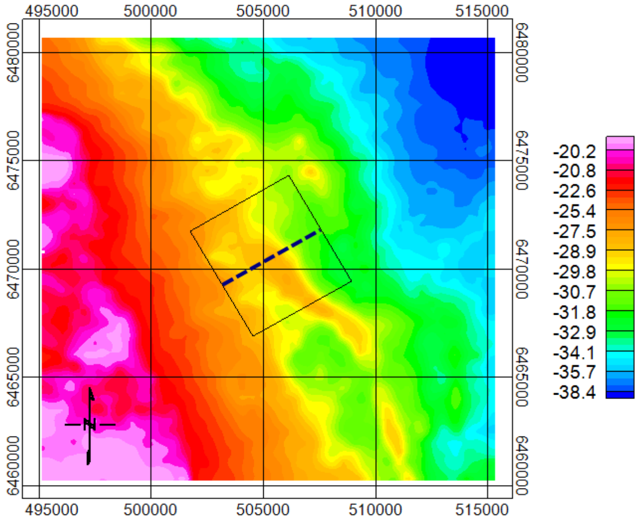


**Figure 5.1: The Kauring regional gravity data in mgal. The black rectangle shows the boundary of our AGG inversion domain. The black dashed line indicates the position of the section views (Line A)**

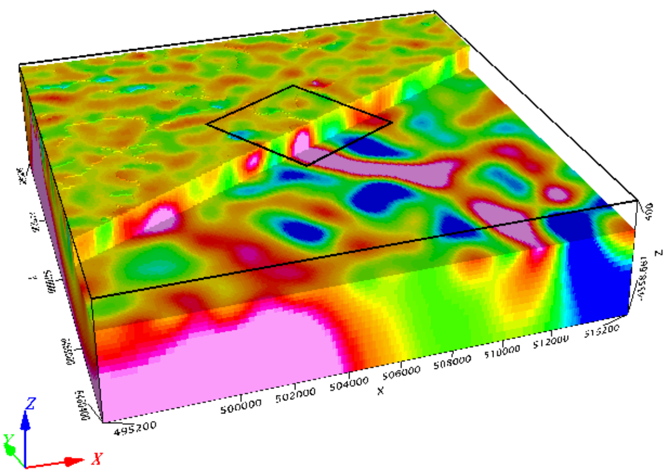


**Figure 5.2: The gravity model recovered by inversion of the regional gravity data in Figure 5.1. The black rectangle shows the boundary of the AGG inversion domain.**

Although it is not required by our method for gravity referenced gravity gradient inversion it is prudent and instructive to compute the AGG response from the gravity model. The result of this forward modelling is shown in Figure 5.3 for the survey line corresponding to dashed line in Figure 5.1 (Line A) as the $G_{XY}$_FWD and $G_{UV}$_FWD channels. Also shown are the corresponding AGG measured channels. There are several interesting aspects to these profiles: first, for the NE component (upper) profile the gravity model generates a good representation of the regional response; second, for the UV component (lower) panel the measured A/B_2p67_UV channels are offset above the corresponding gravity model AGG response by ~10Eo, which is highly suggestive of a systematic error in the AGG data. Third, the gravity model is contributing a regional behaviour which is much more reasonable geophysically than a simple linear trend.

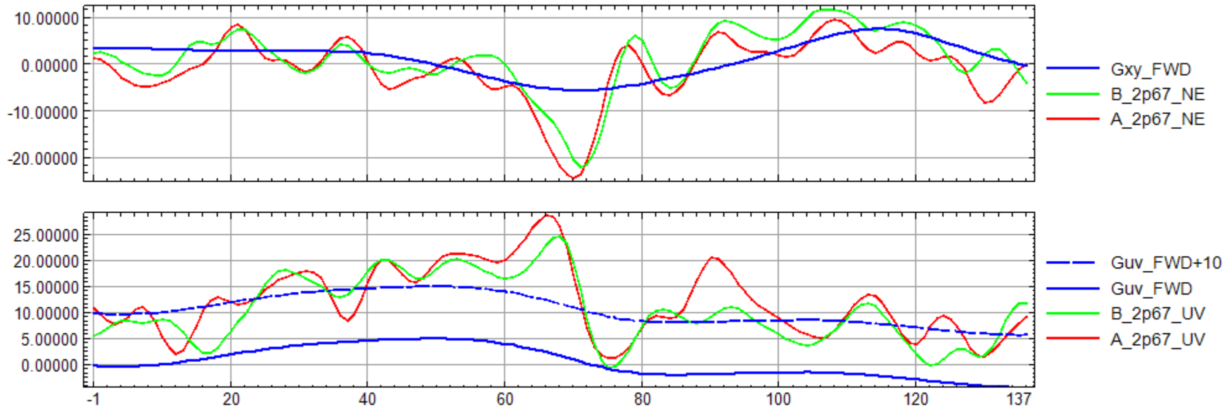


**Figure 5.3: For Line A, the observed AGG A/B_2p67_NE/UV (A-red, B-green, NE-upper, UV-lower) profiles in Eo. The $G_{NE}$ and $G_{UV}$ responses predicted from the gravity derived density model shown in Figure 5.2. The dashed blue line is the $G_{UV}$ predicted response plus 10 Eo indicating the systematic bias in the measured data.**

The result of the gravity referenced AGG inversion is shown in Figures 5.4a-e: (a) the surface density; (b,c,d) horizontal sections at 250m, 150m, and -150m elevations which correspond approximately to 100m 200m and 500m below surface; and (e,f) are a section through the primary density anomaly at y=3000m (Line A) shown with two different colour scales. These density images should be compared to those of Figures 4.2a-f keeping in mind that the only difference in the inversion inputs is the use of the gravity derived density reference model and mean data background removal rather than the "conventional" default zero density reference model and linear trend removal. Figures 5.4a-e share the colour scale shown in Figure 5.4e. Figure 5.4f shows the same section as 5.4e but with a linear colour scale to emphasize the high density target.

## DISCUSSION

A comparison of inversion results at Kauring between the "conventional" inversion (Figures 4a-e) and gravity referenced gravity gradient G-GG inversion must always be somewhat subjective because technically both models fit the data to exactly the same level, 3.5 Eo. However we believe the G-GG inversion model is preferable from an interpretation perspective because it shows density domains more clearly than the "conventional" inversion which focuses attention more on the edges between domains. When there is noise in the data, edge emphasis becomes a little distracting whereas domains maintain better integrity. At the very least, for those who prefer the "conventional" model we suggest that the G-GG model is certainly worth adding to the suite of results that go into a complete exploration interpretation.

Focusing specifically on comparing the "conventional" and G-GG approaches in locating the high density target we recall that in the synthetic model example the location of the target body was significantly improved with the G-GG method over the "conventional" inversion results. In the Kauring field data example the effect on the main anomaly is less pronounced (see Figure 5.5) however in the opinion of the authors the G-GG method gives a slightly better inversion result: the "conventional" inversion yields a target which indicates some dip but also has a tendency to extend vertically deep into the section which can sometimes be an inversion artefact. The G-GG inversion gives a more compact target with more definitive dip. Of course from a real world perspective the difference would probably not affect exploration decisions or geologic interpretations in this case.

The gravity referenced gravity gradient G-GG inversion we have presented is an example of using the gravity inversion output to supply prior information to the gravity gradient inversion and it is the manner in which this prior information is incorporated which is the key to the success of the method. By comparison an alternate approach would be to use the gravity gradient response from the gravity model as a regional gravity gradient response and to perform a regional-residual separation by simple subtraction in the data domain, then invert the residual gravity gradient data. In principle, because of the linearity of the inverse problem, a full density model which fits the data could be recovered by addition of the density models from the gravity inversion and the residual gravity gradient inversion, however, this approach yields inferior results. The reason is that both inversions tend to produce compact density zones and adding compact density zones will produce an artificially structured composite model. Conversely, as shown in the G-GG inversions, using the gravity model as a reference model produces a model without structural artefacts. This is what was alluded to in the introduction about the whole being more than the sum of the parts.

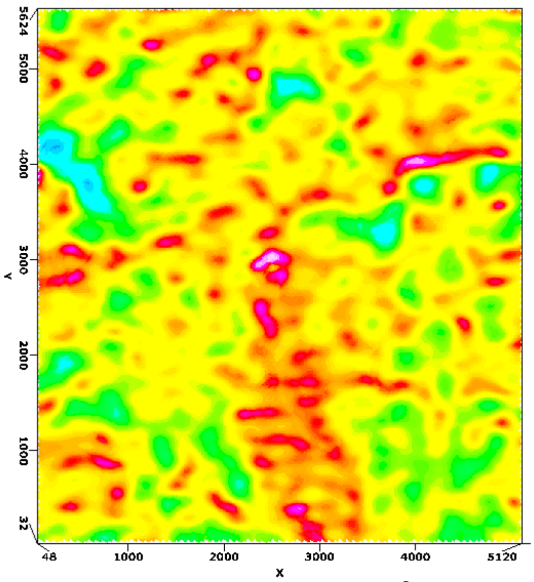


**Figure 5.4a: The surface density (g/cm$^3$) from the gravity referenced AGG inversion.**

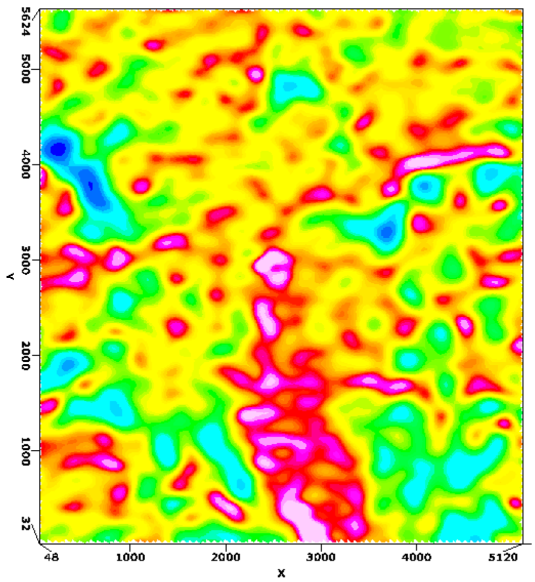


**Figure 5.4b: A density slice at elevation 250m from the gravity referenced AGG inversion.**

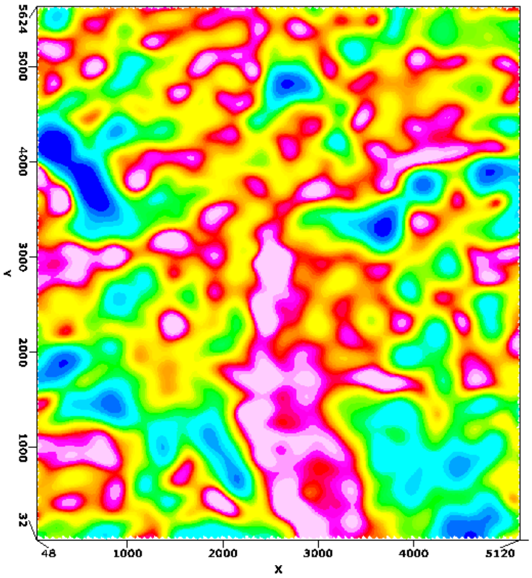


**Figure 5.4c: A density slice at elevation 150m from the gravity referenced AGG inversion.**

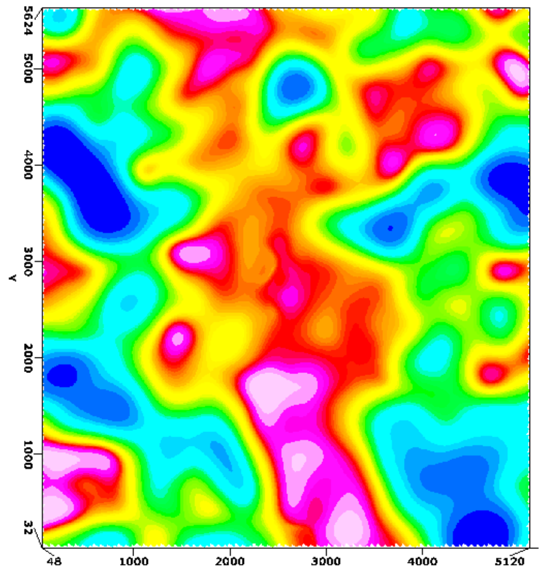


**Figure 5.4d: A density slice at elevation -150m from the gravity referenced AGG inversion.**

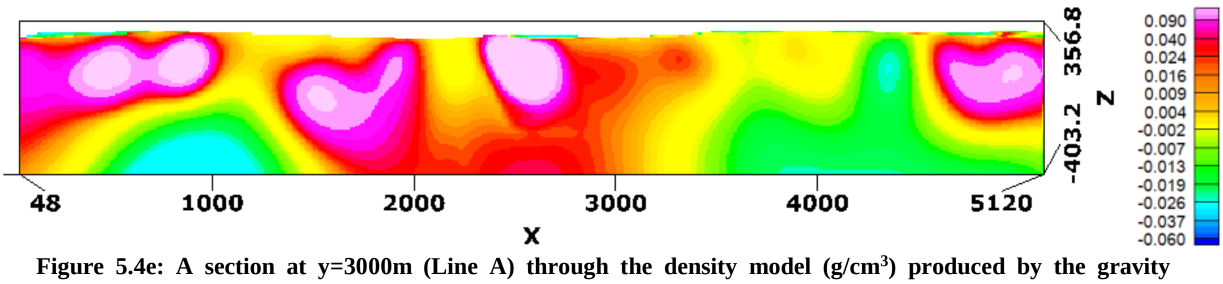


**Figure 5.4e: A section at y=3000m (Line A) through the density model (g/cm$^3$) produced by the gravity referenced AGG inversion. A histogram equalized colour scale is used to convey the general structure of the model.**

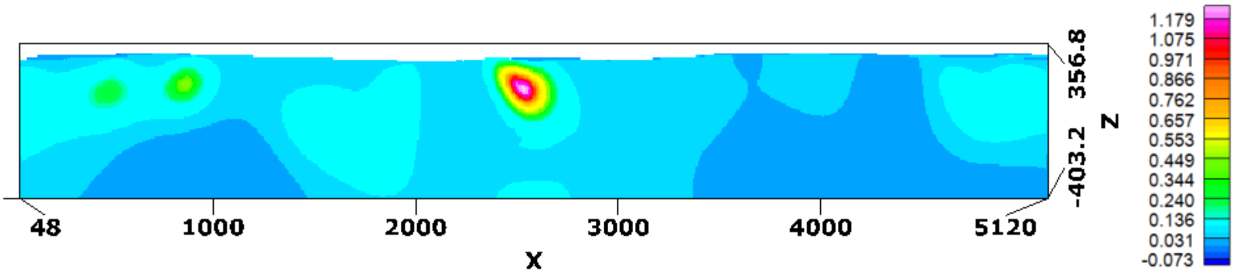


**Figure 5.4f: A section at y=3000m (Line A) through the density model (g/cm$^3$) produced by the gravity referenced AGG inversion. A linear colour scale is used to convey the structure of the high density target.**

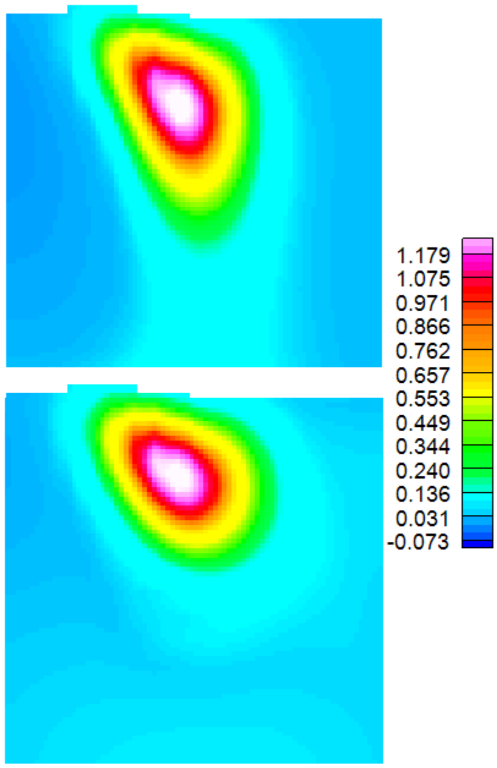


**Figure 5.5: A magnified view of the anomaly in Figures 4.2f and 5.4f comparing the density (g/cm$^3$) models from "conventional" inversion (upper) with the gravity referenced gravity gradiometer G-GG inversion (lower).**

## CONCLUSIONS

In exploration areas where there are both gravity gradient data and regional (or detailed) gravity data it is important to incorporate both data types to produce a density model which benefits from the strengths of each data type. To this end we have presented a gravity referenced gravity gradient G-GG inversion method: the first step is to invert the regional gravity data to produce a regional density model, followed by a gravity gradient inversion using the regional density model as prior information incorporated through a "reference model". The method is efficient and effective. We demonstrated the G-GG method on a synthetic model and addressed the close relationship between using the gravity model as prior information in the gravity gradient inversion and gravity gradient regional-residual separation. For the synthetic case the G-GG method produced much better target location than "conventional" inversion. We applied the G-GG method to Falcon™ AGG data collected over the Kauring test site and regional gravity data sampled on a 500m grid. The G-GG method decouples the gravity inversion from the gravity gradient inversion so that any irregular or sparse sampling in the gravity data does not conflict with the higher sampling rate of the gravity gradient data. We observed that the gravity gradient response from the gravity model produced a good regional response for the $G_{NE}$ Falcon™ channels, however it suggested a 10 Eo systematic offset in the $G_{UV}$ channels. This data offset must be corrected before any inversion can be undertaken. While this forward modelling is not necessary for the G-GG method it does provide a useful validation of the gravity gradiometer data, and is strongly recommended when gravity data are available. The results from the G-GG inversion produced, in the opinion of the authors, a more easily interpretable density model than "conventional" inversion. The G-GG inversion showed density domains more clearly than the "conventional" inversion which focused attention more on the edges between domains. When there is noise in the data, edge emphasis becomes a little distracting whereas domains maintain their integrity better consequently making interpretation more straightforward. For targeting purposes, while the synthetic example showed a significant improvement when using the G-GG method, for the Kauring test site the G-GG inversion showed a small improvement in the target image. We conclude that for exploration mapping and targeting using gravity gradient data, when regional gravity data are available, the G-GG method is certainly worth adding to the suite of results that go into a complete exploration interpretation.

## ACKNOWLEDGMENTS

The authors would like to sincerely acknowledge the inspiration and effort of all involved in developing the R.J. Smith Kauring Test Site datasets.

## REFERENCES

Bates, M., and S. Elieff, 2012, Technical Report - Kauring Gravity Test Site - Western Australia, 2012, for Victoria State Government Department of Primary Industries: Unpublished Sander Geophysics Limited report.

VOXI, Geosoft Inc., www.geosoft.com/products/voxi-earth-modelling/overview

Howard, D., M. Gujic, and R. Lane, 2010, The Kauring airborne gravity and airborne gravity gradiometer test site, Western Australia: in RJL Lane (editor), Airborne Gravity 2010 Abstracts from the ASEG-PESA Airborne Gravity 2010 Workshop: Published jointly by Geoscience Australia and the Geological Survey of New South Wales, Geoscience Australia Record 2010/23 and GSNSW File GS2010/0457, pp. 107-114

Lane, R., M. Grujic, T. Aravanis, R. Tracey, M. Dransfield, M, D. Howard, and B. Smith, 2009, The Kauring Airborne Gravity Test Site, Western Australia: Eos Trans. AGU Fall Meeting Supplement, vol.90, Abstract G51A-0656.

Lee, J. B. 2001, FALCON gravity gradiometer technology, Exploration Geophysics, 32(3/4), 247-250

Zhdanov, M. S., R. G. Ellis, S. Mukherjee, 2004, Three-dimensional regularized focusing inversion of gravity gradient tensor component data, Geophysics 69(4), 925-937.